SensMiLi:
Optical Absolute Position-Encoder
by Single-Track, *q*-ary Pseudo-Random-Sequences for Miniature Linear Motors

Wibbing, D.*[a], Binder, J.[a], Schinköthe, W.[b], Pauly, Ch.[c], Gachot, C.[c], and Mücklich, F.[c]
[a]Festo AG & Co. KG; [b]IKFF, University of Stuttgart; [c]LFW, Saarland University
*[a]Ruiter Strasse 82, 73734 Esslingen, e-mail: dwb@de.festo.com, phone: +49 711 347 50861

Abstract: *A novel principle for an optical absolute position encoder is presented, which is based on the diffraction of light. Optimized for the integration into miniature linear motors, the encoder is designed to enable highly dynamic, micrometer precise positioning in clean room environments. Whereas to the author's knowledge pseudo-random-sequences in position encoders have so far only been realized by binary imaging techniques, now for the first time they are implemented by optical diffraction. On the one hand this opens up the possibility for a higher code-efficiency by q-ary coding and on the other hand it allows less stringent focusing restrictions. The single tracked scale consists of a sequence of gratings, which diffract the Gauss-shaped spot of a laser diode and reflects it onto a sensor matrix. The two-dimensional locations of the diffraction spots are decoded to obtain the position information, which can be refined below the width of the gratings by evaluating the intensity distribution across these spots. An experiment shows how the scale can directly be written onto the stainless steel piston-rod of the motor by Focused Ion Beam writing.*

1 Introduction

In segments of automation industry like the semiconductor, the electric light assembly or the biomedical industry small parts have to be handled in clean environments with an acceleration of several hundred m/s² and a precision in the one-digit micrometer range. Miniature linear motors offer the dimensional and dynamical characteristics to fulfil these needs. In order to control the motor's movements, position encoders have to be integrated into their housings. Absolute encoders, that know their position at any time, can safe a significant amount of time at start-up, because they neither require the motor to search its phase of commutation nor require zero-referencing to start the position measurement. However, up to now there has not been a sufficient solution for a precise absolute linear encoder which could have been integrated into such a miniature linear motor. This is why a new position encoder is being developed, which aims to be an integral part of the mechatronic drive system.

2 State of the Art

2.1 Scale-based imaging encoders

State-of-the-art scale-based optical linear absolute position encoders mostly use pseudo-random coded absolute tracks with coarse position information in combination with a parallel or overlaid track of incremental coding to increase their resolution [1; 2]. Binary pseudo-random-sequences (PRS) look similar to the bar-codes known from consumer goods, which code their binary information (e.g. 0100111001) by a sequence of equally spaced black and white lines. This single code track (Fig. 1b) shows two advantages over the formerly used parallel tracks of binary code (Fig. 1a): On the one hand the height of the scale can be reduced if only one track is necessary and it remains the same no matter how many digits the code word includes. On the other hand the tolerance against yaw-angle errors becomes significantly smaller. The sensor-head always reads n consecutive bits of the PRS, which do not occur at a second location in the same sequence on the entire scale. This way, each movement by a single digit results in a new code word.

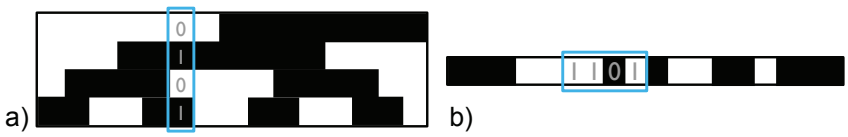

Fig. 1: *a) Parallel coding. b) Serial coding.*

2.2 Scale-based diffractive encoders

Recently a new coding principle has been developed for incremental and absolute rotary encoders, that is not based on imaging dark and bright scale structures on a sensor-matrix any more [3; 4]. Instead, the scale consists of diffraction gratings (Fig. 2a). Illuminating a certain number of these gratings by a laser-diode, the light is diffracted into a pattern of light spots on a sensor plane. The position of these so called diffraction orders can be decoded to retrieve the angular position of the rotary encoder.
One major advantage of this coding principle is its potential robustness against distance changes between scale and read-head (see Δz in Fig. 2c). Unlike the optical micrometer-sized structures on imaging scales (Fig. 2b), those of the diffractive scale (Fig. 2c) do not have to be resolved by a lens-system to obtain the coded information. Instead, the information on the scale is indirectly read from the diffraction pattern it causes. As a consequence, the light does not have to be focused as tight and the depth of focus will be larger. Like this the depth of focus can be decoupled from the resolution and the sensor becomes more robust against distance-changes between scale and read-head.

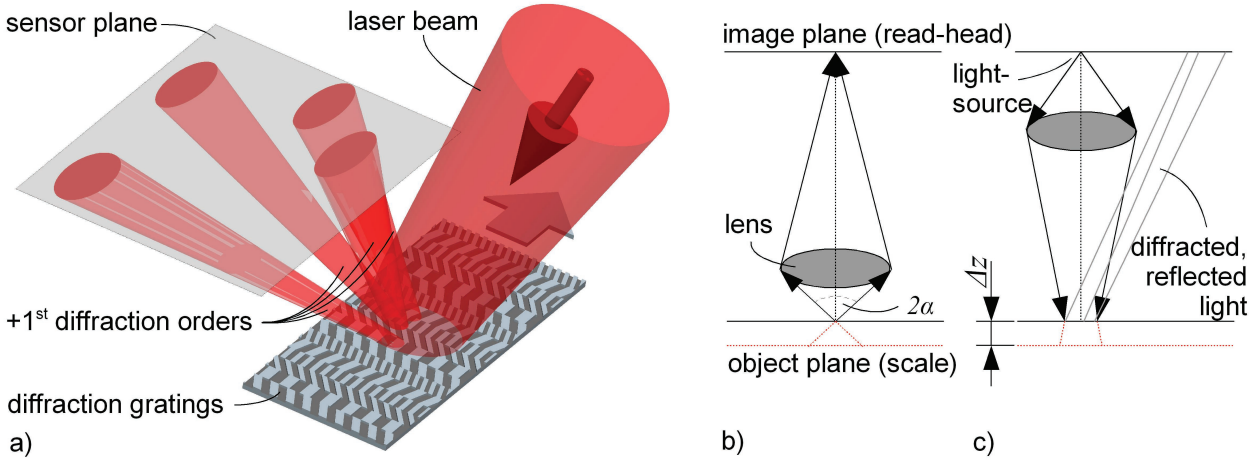

Fig. 2: *a) Schematic drawing of principle of diffractive encoder without 0th diffraction order.*
b) Depth of focus for resolving small structures in imaging optics.
c) Depth of focus when illuminating diffraction gratings.

3 *q*-ary Pseudo-Random-Sequences by Diffraction

Position encoders for linear motors often require a larger quantity of absolute position-information than rotary encoders since their measurement range has to be longer than the circumference of an encoder disc at similar resolution. For this purpose a novel diffractive coding-principle is introduced, which allows to implement more discrete absolute position information on the scale than the serial Gray-Code described in [4]. This coding principle is based on binary pseudo-random-sequences (PRS) introduced in section 2.1 and will be described in the following.

3.1 Basics about the Coding

Pseudo-random-sequences of maximum length $e = q^n - 1$ can not only be obtained for the binary case where q = 2 but for any q, which is a power of some prime and for any positive integer n, by using a maximal Linear-Feedback-Shift-Register (LFSR) [5; 6]. Choosing a q different from 2 can improve the code-efficiency η, which in this work is suggested to be the quotient of the number of code words and the number of different diffraction-spot positions:

$$\eta = \frac{q^n}{q \cdot n} \tag{1}$$

If e.g. q^n >10 000 was needed and the number of diffraction-spot positions should be as small as possible to facilitate their placement, their distinction, and their sensory detection, q = 3 would lead to a better result than q = 2. The code efficiency is also relevant for estimating the complexity and costs of the sensor matrix, since it could e.g. determine the number of required matrix elements.

As described in the following, diffraction gratings can be the key to realize these highly efficient q-ary PRS.

3.2 Basics about Diffraction

Illuminating a single transparent grating, a diffraction-pattern can be observed in the far-field, which is caused by the interference of the coherent light. One portion of the light, called the 0th order, passes right through the grating without being diffracted. Another portion of light will be diffracted into the $\pm m^{th}$ diffraction orders according to the diffraction angle β [7]:

$$\beta = \arcsin\left(\frac{m \cdot \lambda}{g}\right) \tag{2}$$

where m is a natural number, λ is the wavelength of light and g is the grating-period. Since the intensity of the orders will decrease with their increasing number, the sensor will be designed to detect either the +1st or the -1st orders only.

By choosing the period g and the angle γ of a grating, it is possible to determine at which two-dimensional position the diffraction orders hit the image plane. Reading which predetermined positions are hit, the information of the gratings can be decoded.

Designing a sequence of grids to code a pseudo-random-sequence, it might at the first thought appear to be sufficient to implement only one information into each grid. E.g. in a binary code two different grid-angles could encode the digits 0 and 1. However, the information about the sequence of the gratings gets lost in the far-field and it is not possible any more to find out if the code is e.g. “01” or “10”. The novel solution for this problem will be described in section 3.3.

3.3 Encoding and Decoding the Pseudo-Random-Sequence

The coding of a pseudo-random-sequence will be explained by an example shown in Fig. 3. In this example a code word consists of 7 digits each of which can take one of 5 different values. Thus the pseudo-random-sequence contains 5^7 = 78125 consecutive code words, each representing a discrete position. The length of the code word is determined by how many gratings are illuminated by the light-spot. However, the light-spot of a laser-diode does not have a sharp edge, but rather a Gauss-shaped intensity-distribution which consequently can be observed across the orders of the diffraction-pattern as well.

To retrieve the information about the sequence of the gratings, i.e. the position of the digits within the code word, the vertical position of the diffraction orders on the sensor plane is varied. This is done mainly by adjusting the period of the gratings. Like this, each position of a digit within a code word will be mapped to a different row of the sensor-matrix. The variation of the grating-periods is done cyclically along the whole scale and the length of this cycle equals the word-length + 2. In the example, this means that the grating period continuously increases over 9 gratings and then starts with the smallest grating period again like shown in Fig. 3 above the gratings in the second row of numbers. To obtain the 7 gratings, which belong to the code word, the most intense column in each of the 9 rows has to be detected. Out of these 9 matrix-elements, the 7 most intense have to be chosen. The missing 2 row-numbers will then allow to reconstruct the sequence of the 7 gratings of the code word. In the example,

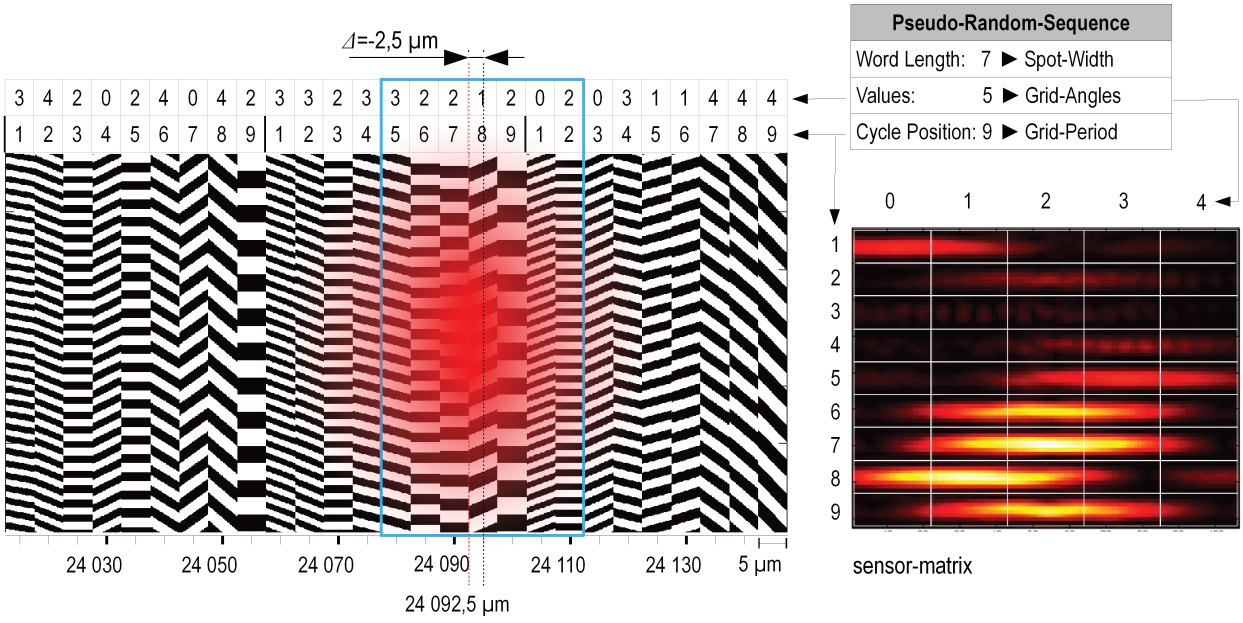

Fig. 3: *Schematic drawing of coding and decoding the pseudo-random-sequence.*

the row numbers of the 7 most intense matrix-elements are 1, 2, 5, 6, 7, 8, and 9, which means that row 3 and 4 are missing. The two missing rows, i.e. the two missing gratings, can not originate from within the illuminated region, but only from its borders, since they are the least intense. Consequently the sequence-numbers may not have a gap and thus must be arranged in the order 5-6-7-8-9-1-2.

Now that the sequence of the rows, i.e. the sequence of the digits, is known, their values have to be decoded. These have been encoded into the horizontal position of the diffraction orders, which is mainly influenced by the grating angle. The values can thus be read-out by identifying the column number of each of the 7 most intense matrix-elements. In the example, the column numbers, aligned in the row sequence 5-6-7-8-9-1-2 as detected above, are 3-2-2-1-2-0-2. This is the code word that had to be detected from the diffraction pattern.

Decoding the position value from this code word can be done by searching the value pair in a look-up table. If in this table the code words are stored in the sequence of their corresponding decimal value, the value-pair can directly be found by calculating the decimal value of the current code word. In the example the position-value paired with the code word is 24095 µm.

3.4 Improving the Resolution

Up to now the resolution of the measurement is limited to the width of a grating, which in this example is 5 µm. Experiments showed that it is difficult to go below this value, because the thinner the diffraction-gratings are in the vertical, the longer the diffraction spots will get in the horizontal and the more difficult it will become to detect their horizontal position. To increase the resolution, though, the Gauss-shaped intensity distribution across the diffraction orders can be made use of . For this purpose the most intense columns per row of the sensor-matrix are aligned sequentially and are spaced by the distance of their gratings on the x-axis (see Fig. 4 c). This way the diffraction orders are mapped to the geometrical arrangement of the gratings they belong to. Therefore, the cycle length of the grating sequence information has to be longer than the code word by 2 digits. If it was only longer by 1 digit, then it would not be possible to determine whether its grating would be at the front or at the back of the gratings of the code word. Finally a Gaussian regression curve is fitted to their intensity-values in order to obtain the x-coordinate of the peak-value of this curve. By previously assigning a position-value to each code word like described in section 3.3, it was assumed that the centre of the illumination-spot would be identical to the centre of the grating in the middle of the code word. Now this assumption can be corrected by the difference Δ between the x-coordinates of the Gaussian peak-value and the grating in the middle of the code word. Thus a resolution in the sub-grid range can be achieved. In the example of Fig. 3 the spot centre is 2.5 µm to the left of the grating that is in the middle of the code word, so the improved position-value is 24092.5 µm.

3.5 Relaxing the Scale-Requirements

Ideally the relation between the grating period g and the height of the spaces b should be 1/2. In this special case the intensity of all even diffraction orders will be zero and thus especially the 2nd order will not be able to interfere with any of the other grating's 1st diffraction orders within the sensor area. However, already a slight deviation from this ratio will allow the even orders to emerge. This can be explained by a simplified formula for the intensity distribution I of the diffraction orders as a function of the diffraction angle β like derived in [7]:

$$I(\beta) = I_0 \left(\frac{\sin \psi}{\psi} \right)^2 \cdot \left(\frac{\sin(N\xi)}{\sin \xi} \right)^2 \tag{3}$$

with $\psi = \frac{kb}{2} \sin\beta$, $\xi = \frac{kg}{2} \sin\beta$, $\sin\beta = \frac{m\lambda}{g}$, $k = \frac{2\pi}{\lambda}$ and N: number of slits

Setting m to an even number and $g = 2b$, the intensity will always be zero.

Manufacturing the scale sufficiently precise, so b/g would not deviate from 1/2 significantly, could be a difficult task. For this reason the 1st diffraction orders should be placed on the sensor-matrix so the 1st and 2nd orders will not interfere. A first approach to solve this task by geometrical considerations is shown in Fig. 4b.

4 Verification of Functionality

After the diffraction pattern and its decoding has been simulated and optimised in Matlab, the real

behaviour of the grating sequence shall be verified in an experiment. Therefore the grating-sequence is structured into a chrome-layer on a glass substrate by a circular laser writing system [8] at the Institute of technical Optics at the University of Stuttgart. These light-transmissive amplitude gratings are illuminated by an 855 nm VCSEL diode (vertical cavity surface emitting laser), the light of which is focused by a 2 mm ball lens to form a spot of about 50 µm in diameter. A camera is used to sense the diffraction pattern and to send it to the computer. Matlab reads in the image like shown in Fig. 4a, cuts out the region of interest, lays the sensor matrix over it (Fig. 4b), and evaluates the matrix elements to decode the circumferential position of the rotary scale.

The PRS used in Fig. 4 is based on a ternary code which has a word length of 9 digits, thus being able to code 3^9 = 19683 positions with $3 \cdot (9 + 2) = 33$ photo-diodes. At a grating width of 5 µm this corresponds to a measurement range of 98.415 mm.

Since in this first simple experiment the glass substrate could only be rotated manually by a micrometer screw, norm conform measurements could not be conducted yet. Nevertheless, a verification of the basic functionality and an impression of the achievable performance can already be gained. A measurement of the linearity error over a distance of 35 µm showed a result of 0,419 µm and the worst of three exemplary measurements of the repeat-accuracy showed a maximum difference of 0,5 µm between 20 repeated measurements.

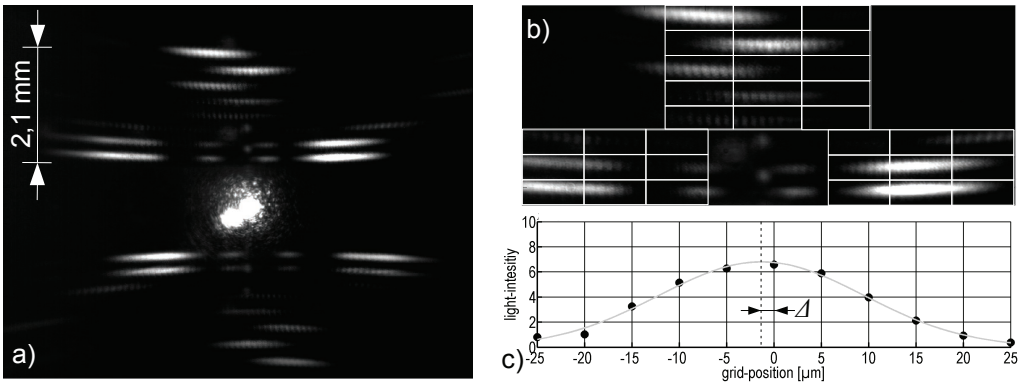

Fig. 4: *a) Diffraction pattern observed with experimental set-up. b) Cut-out of a) with sensor-matrix. c) Gaussian regression over most intense matrix-elements per row in b).*

An important deviation between measurement and simulation is, that the maximum intensities of the $\pm 1^{st}$ diffraction orders are not the same. The steeper the grating angle the smaller the illuminated number of grid-lines will be and the lower the maximum intensity of the corresponding diffraction-order will be. To compensate this effect, the maximum intensities of each type of grating (33 in this example) can be measured and multiplied by a correction factor.

5 Direct Structuring of the Scale in Steel

For the integration of the position-encoder into a linear motor, it is a significant advantage to directly structure the scale onto the steel of the motor's piston-rod. On the one hand, no extra scale tape is needed that would require a mechanically complex assembly and a temperature resistant linkage. On the other hand, a measurement error, resulting from temperature changes, could be corrected more easily than if two different materials with two different coefficients of expansion would be expanding against each other.

It is very difficult to realize these gratings with periods as small as 2 µm in stainless steel, since the hardness of the material requires to focus a lot more energy onto the processing area than would be necessary for e.g. silicon. To investigate if this is possible at all, a Focused Ion Beam writer is employed.

The Focused Ion Beam method (FIB) has proven to be a flexible tool for the fabrication of surface structures on the micrometer and sub-micrometer scale [9, 10]. Modern FIB/SEM systems have different ways for writing complex structures onto sample surfaces, such as CAD interface software, stream files, ion beam lithographic systems and, used in this work, direct bitmap import. Structuring was performed using a FEI Helios Nanolab600 FIB/SEM workstation featuring a high resolution SEM combined with a Ga ion column. This system uses 24 bit windows bitmap files (.bmp) where the value of the blue channel of each individual pixel is translated into an ion beam dwell time. The bitmap resolution has to be fitted to the ion beam diameter of the aperture used for structuring to make sure that the ion dose is uniform in the

x,y-plane. Wrong parameters would instead result in a dot-like pattern. Finding the correct ion beam current requires the consideration of two adverse effects. On the one hand, low currents are best for milling small features as the beam diameter decreases with decreasing beam current. On the other hand, this will greatly increase the total milling time resulting in susceptibility to sample drift and inefficient use of the workstation. A comparison of different milling parameters has shown that a beam current of 2800 pA is an acceptable compromise between resolution and milling time. For improved accuracy, an auxiliary software module is used to correct sample drift during milling.

This way, a test-structure of 12 gratings has been manufactured on stainless steel at the Chair of Functional Materials at the Saarland University (Fig. 5b). By illuminating these gratings with a VCSEL diode (Fig. 5a), a diffraction pattern can be observed (Fig. 5c), which would enable the decoding of the position information in a quality comparable to that one which has been demonstrated in Fig. 4 by the transmissive chrome grating.

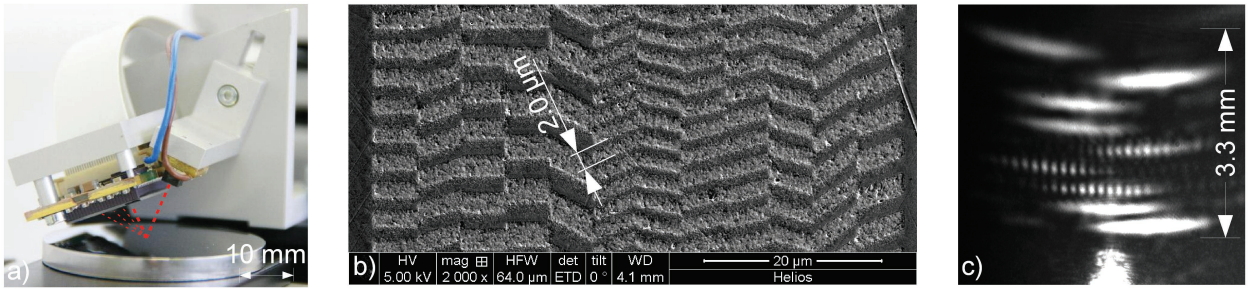

Fig. 5: *a) Experimental set-up with laser-diode, steel test piece and camera-sensor. b) REM image of 12 diffraction-gratings on test piece of a). c) Diffraction-pattern observed in a).*

6 Conclusion

A novel principle for an optical absolute position encoder has been developed, which allows to realize highly efficient q-ary pseudo-random-sequences by diffraction gratings. Evaluating the diffraction pattern of these gratings, the resolution can be decoupled from the depth of focus, so, compared to imaging encoders, a better tolerance for distance-changes between read-head and scale can be achieved. The key components of this encoder are optimized for the use in miniature linear motors: The sensor can consist of a matrix of only a few photo-diodes, which allows a fast parallel read-out and a simple position decoding. The optical system only consists of a laser-diode and a lens, which enables a space-saving integration into the motor. The scale can be structured directly onto the steel of the motor's piston-rod, thus facilitating the manufacturing process and improving the temperature tolerances. First experiments demonstrated that a sub-grid resolution with the potential for a linearity as well as a repeat-accuracy in the range of 0.5 µm can be achieved.

7 References

[1] Heidenhain GmbH, Datasheet and Website, http://www.heidenhain.de (2011).

[2] Renishaw plc, Datasheet and Website, www.renishaw.com (2011).

[3] Hopp, D., Pruß, Ch., Osten, W., Seybold, J., Mayer, V., and Kück, H., „Optisch Inkrementaler Drehgeber in Low-Cost-Bauweise“, Technisches Messen, Oldenburg Wissenschaftsverlag, 6/2010.

[4] Hopp, D., Pruß, Ch., Osten, W., Seybold, J., Mayer, V., and Kück, H., „Drehwinkelsensor“, AiF Abschlussbericht 219 ZN, 2008.

[5] Schroeder, M., “Number Theory in Science and Communication”, 8th edition, Springer, 2008.

[6] Balle, B., Ventura, E., and Fuertes J. M., “An Algorithm to design prescribed length codes for single-tracked shaft encoders”, Proc. of the 2009 IEEE Int. Conf. on Mechatronics, Spain, 2009.

[7] Univ. Wuppertal, “Phys. Anfängerpraktikum für Studenten der Chemie, Versuch WO1-Ch, Beugung und Interferenz von Laserlicht”, 2006, www.delphi.uni-wuppertal.de/~kind/wo1ch.pdf (2011).

[8] Poleshchuk, A., G., et al., “Polar coordinate laser pattern generator for fabrication of diffractive optical elements with arbitrary structure”, Applied Optics, Vol. 38, No. 8, 1999.

[9] Wilhelmi, O., Reyntjens, S., Mitterbauer, C., Roussel, L., Stokes, D.J., and Hubert, D.H.W., “Rapid Prototyping of Nanostructured Materials with a Focused Ion Beam” Japanese Journal of Applied Physics, Volume 47 (2008), pages 5010-5014

[10] Holzapfel, C., Schäf, W., Marx, M., Vehoff, H., Mücklich, F., “Interaction of Cracks with Precipitates and Grain Boundaries: Understanding Crack Growth Mechanisms through Focused Ion Beam Tomography“, Scripta Materialia, 56(2007) , 0, 697-700